PROCEEDINGS, 42nd Workshop on Geothermal Reservoir Engineering
Stanford University, Stanford, California, February 13-15, 2017
SGP-TR-212

Automatic Moment Tensor Analyses, In-Situ Stress Estimation and Temporal Stress Changes at The Geysers EGS Demonstration Project

Douglas S. Dreger[1], O. Sierra Boyd[1], and Roland Gritto[2]

[1]Berkeley Seismological Laboratory, Berkeley, CA, 94720

[2]Array Information Technology, 2020 Cedar Street, Berkeley, CA 94709

Roland.Gritto@arrayinfotech.com

Keywords: EGS development, fracture characterization, moment tensor analysis, stress state and temporal changes

ABSTRACT

We investigate seismicity in the vicinity of the EGS development at The Geysers Prati-32 injection well. The goals of our study include the ability to estimate the activated fracture area and volume, to estimate stress drop and stress drop changes as well as fluid saturation and temporal changes in fluid distribution. In this study, we have developed an automated moment tensor analysis technique applicable to earthquakes M≥1.0 to obtain sufficient earthquake source parameters for subsequent in-situ stress estimation and temporal changes during the injection phases. The result of our effort has been the compilation of a 168-event waveform-based seismic moment tensor catalog for events ranging in moment magnitude from 0.7 to 3.7. The moment tensor catalog was subsequently used to invert for the stress tensor, and to investigate possible temporal changes resulting from the fluid injection. The results demonstrate the quality of the seismic moment tensor catalog through the relatively small uncertainties in the recovered stress tensors. We find that there is an approximate 15-degree counterclockwise rotation of the least compressive stress σ3, and a rotation of the maximum compressive stress σ1 toward the vertical as the injected volume of water increased. The magnitude of these rotations is consistent with other nearby empirical observations (Martinez-Garzon et al., 2013) and thermo-hydromechanical simulation results (Jeanne et al., 2015). We find that there is a systematic reduction in the stress shape factor, R, as the injected water volume increases, indicating an evolution toward a more tensile stress state.

1. INTRODUCTION

Identifying, creating, and managing fractures and flow paths are essential tasks during EGS resource development. The successful generation of a fracture network requires a priori knowledge of in-situ stress and natural fracture orientation and spacing, among others. However, because the orientation and magnitude of in-situ stress may not be reliably available and injecting fluids at high rates and volume may disturb the natural stress state, it is advantageous to monitor in-situ stress during the injection process. Knowing the stress evolution, the size of the fractures and the nature of the rupture process, as well as the spatial distribution of the fluid flow are essential to control the generation of the fracture network. Our ongoing research addresses these issues by developing an integrated technology approach, to estimate in-situ stress, size of the generated fractures, and spatio-temporal fluid distribution during reservoir stimulation.

Our research goal is to improve technology to assess in-situ stress magnitude and orientation, kinematic fracture parameter, rupture size, as well as temporal and volumetric distribution of the injected fluid during Enhanced Geothermal System (EGS) resource development. We leverage high-frequency seismic data recorded by the LBNL 34-station permanent geophone network and seismic broadband data recorded by a temporary 33-station seismometer network that operated in The Geysers during the injection phase of the DOE GTO funded EGS demonstration project at Prati-32. The operation of the broadband network with high station density and azimuthal coverage to monitor the injection phase produced an unprecedented dataset that is typically unavailable for EGS operations. The two datasets offer two main advantages. (1) The parameters under investigation can be studied over a broader frequency band and at distinct sensitivity levels and (2) the higher sensitivity of the broadband seismometers resulted in a richer dataset with a lower magnitude of completeness.

A first step for both inverting for in situ stress and for developing a source-area scaling relationship is the development of a robust seismic moment tensor catalog. Using waveform data from the LBNL short-period network we have refined a semi-automated approach for estimating the seismic moment tensor and have compiled a 168-event seismic moment tensor catalog for events ranging in moment magnitude from 0.7 to 3.7. In the following, we present our work on estimating in situ stress and temporal stress changes throughout the injection phase at Prati-32.

2. DEVELOPMENT OF A MOMENT TENSOR CATALOG

The Geysers geothermal reservoir in northern California is the largest geothermal reservoir in the world with approximately 1.6 GW installed electric capacity and current production of about 750 MW. The Geysers are located in northern California, USA, approximately 150 km to the north of San Francisco. The region around Prati-32 in the northwest Geysers is presented in Figure 1, which shows the study area, with the locations of the Prati-32 injection well, nearby seismic stations, and known faults.

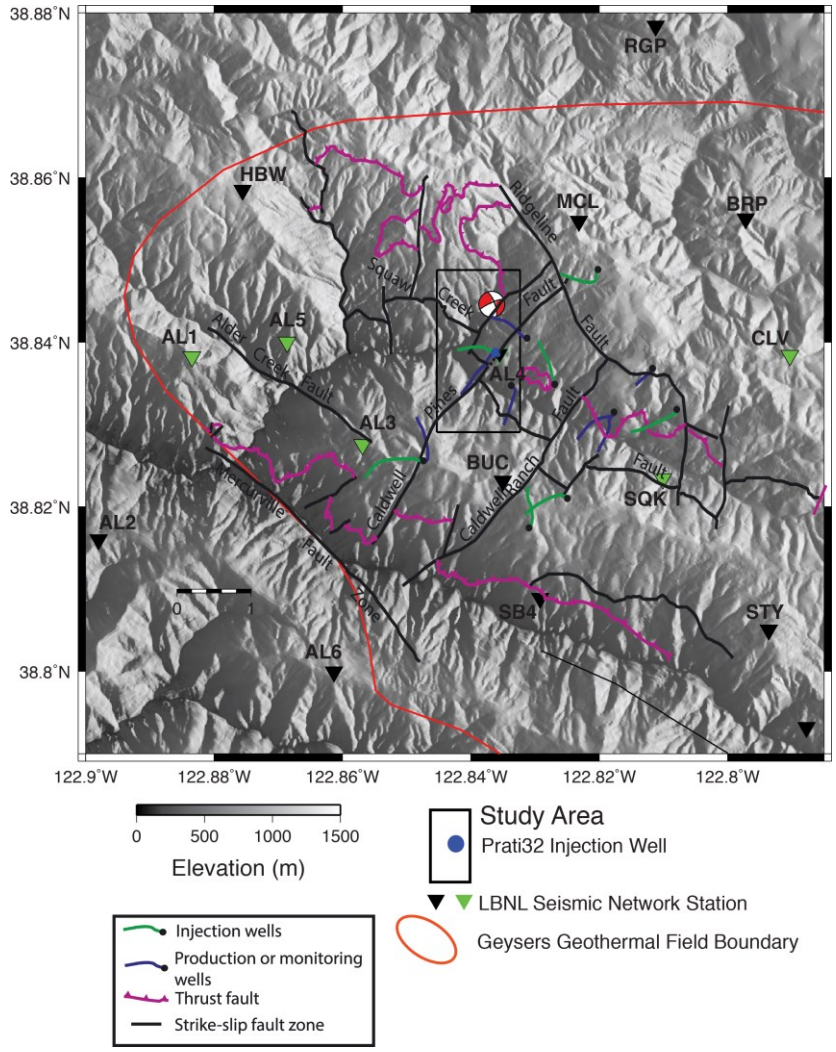

Figure 1: Map showing study area (1x2 km rectangle), Prati-32 well, LBNL seismic stations, and faults.

The timeline of the 168 moment tensor solutions that we obtained from three-component waveform inversion (Gritto et al., 2016) is presented in Figure 2 together with the Prati-32 fluid injection rate. There is a marked increase in both the frequency and magnitude of events following the injection of fluid. The largest events appear correlated with changes in injection rate. During the 2012 injection hiatus the frequency and magnitude of events was seen to decrease.

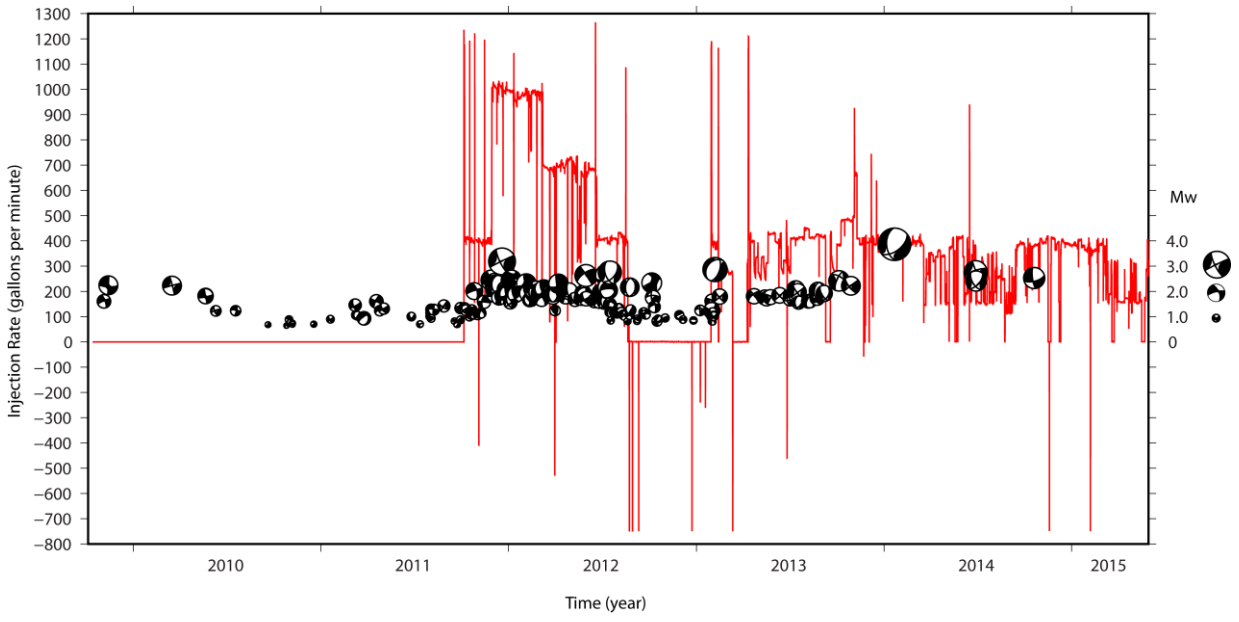

Figure 2: Seismic moment tensor solutions plotted with the 30-day Prati-32 injection rate.

Comparing the monthly averaged injection rate with monthly averaged seismicity (Figure 3) reveals a very strong correlation, in which the low pre-injection rate of seismicity is markedly increased with the initiation of injection. After the injection rate stabilizes the rate of earthquakes is seen to reach a steady level as well. In fact, short-term fluctuations in the injection rate seem to also be marked by short-term fluctuations in the rate of earthquakes. As presented in Figure 2, the magnitudes of these events tend to be very small although a number of M 3+ events have occurred.

We also find that most of the 168 events in our catalog are strike-slip, followed by normal, and a few reverse faulting events (Figure 4). The strike-slip events are found to occur at all depths, whereas the normal and reverse events tend to occur above and within the reservoir. There is also a suggestion that the variety in focal mechanisms is greater prior to and during the first ten months of injection. Subsequent focal mechanisms following multiple shut-in periods become more uniform and consistent with the tensile stress direction inferred from previous studies (Ross et al., 1996; Guilhem et al., 2014; Boyd et al., 2015, 2016).

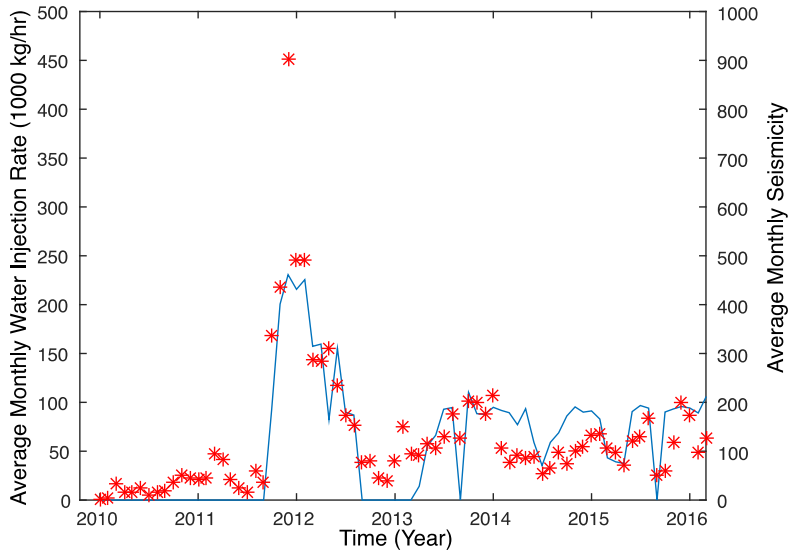

Figure 3: Injection rate (1000 kg/hr, blue line) and EGS Berkeley Geysers average monthly seismicity (red asterisks) as a function of time.

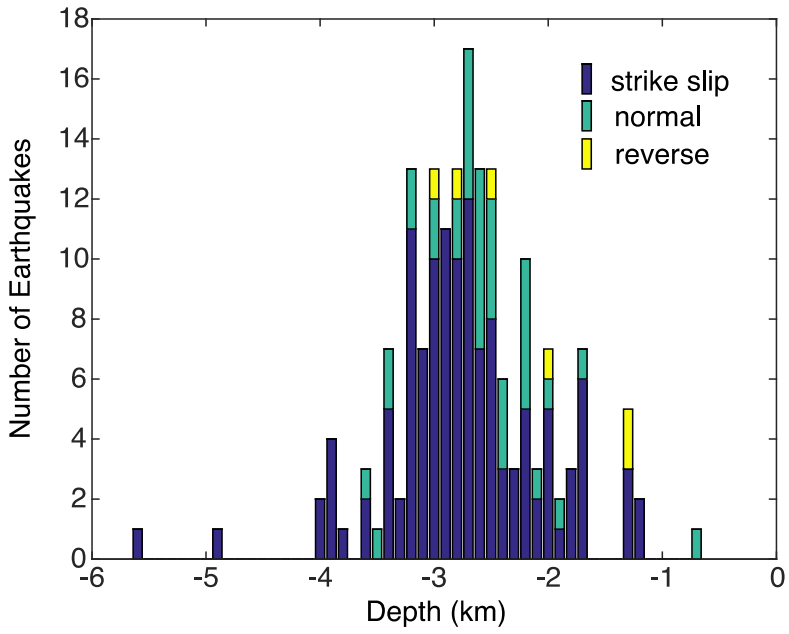

Figure 4: Histogram of fault type determined from our moment tensor catalog as a function of depth. The vast majority of events are of the strike-slip type, followed by normal events (23%), and a few reverse events.

It is observed that our waveform moment tensor based Mw matches that of the LBNL catalog Mw (Figure 5) well, after corrections have been taken to account for the different processing steps. LBNL computes Mw by averaging the instrument corrected P-wave displacement spectrum from 1 Hz to the corner frequency for M<3.5 events, applying the whole space Green's function equation for direct P-waves. Thus, even though both measures are effectively Mw one is computed using the complete waveform including P, S and surface waves and the other only the P-wave displacement spectrum. With our catalog of moment tensors, we will be able to empirically calibrate a spectral estimate of scalar moment and Mw, which we will use during the next year, when we develop a rupture area scaling law to estimate the seismic fracture density of the Prati-32 EGS swarm.

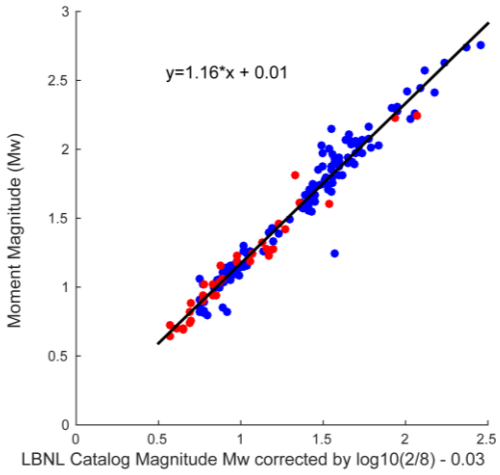

Figure 5: Moment tensor catalog Mw versus LBNL EGS Geysers catalog Mw for pre-injection (red) and injection (blue) events. The slope of linear fit between the waveform and LBNL Mw estimates is close to 1 with a zero intercept indicating good agreement between the waveform and corrected LBNL Mw estimates.

3. IN-SITU STRESS INVERSION

We have used the moment tensor catalog to invert for the in-situ state of stress within the study region. We utilized both the MSATSI software developed by Martinez-Garzon et al. (2014), which is based on the method of Hardebeck and Michael (2004, 2006), and the STRESSINVERSE software package developed by Vavrycuk (2014). We utilized a sliding window containing 30 events for each time period of the stress inversion in which there was a 10-event overlap between time windows. Because it is not known which of the two possible nodal planes is the actual earthquake rupture plane a random sampling of the nodal planes is bootstrapped to assess the uncertainty in the estimated stress tensors in the MSATSI approach, while in the STRESSINVERSE code and iterative method is used to find the nodal planes most consistent with the stress field given fault frictional properties.

Figure 6 shows the focal mechanisms for the pre-injection time period (November 16, 2009 – September 23, 2011) together with the stress inversion results. This time window spans several years to obtain 30 events during this low seismicity rate period for stable stress inversion results, which show an east-southeast orientation of the minimum compressive stress (blue) and south-southwest maximum compressive stress (red), in a principally strike-slip faulting environment.

We have carried out an analysis of the evolution of the state of stress with time, by performing analyses on 12 time windows, each with 30 moment tensor solutions, and each with a 10 event overlap with adjacent time windows. The results in Figures 7 and 8 show an interesting, systematic change in the orientation and magnitude of the stress environment. First, there is an approximately 15-degree counter-clockwise rotation of σ_3. Secondly, beginning in January 2012 when injection rates where high, and the volume of injected water was becoming large there is a marked rotation of σ_1 toward a more vertical orientation. During this period the magnitude of σ_1 and σ_2 also begin to equalize indicating that the system was evolving to a more tensile environment, in which the mechanisms are comprised of both strike-slip and normal types.

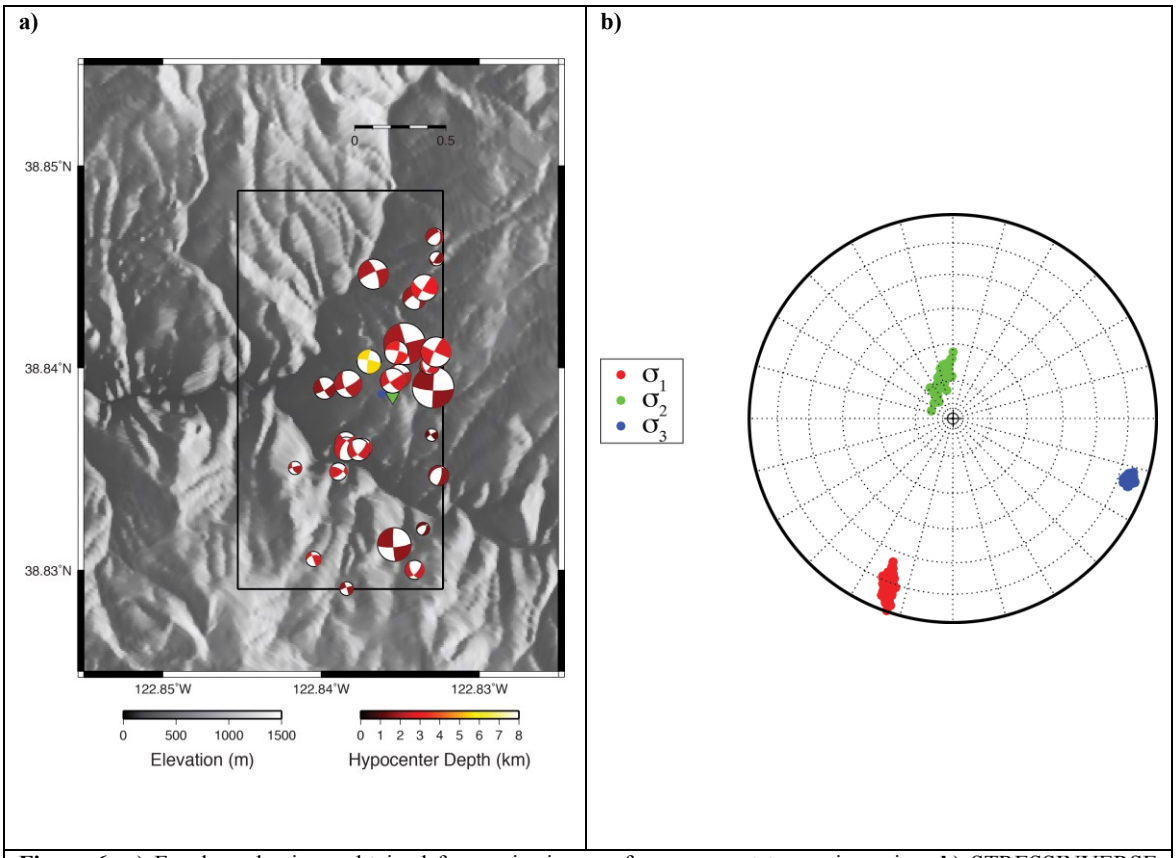

Figure 6: a) Focal mechanisms obtained from seismic waveform moment tensor inversion. **b)** STRESSINVERSE results. σ_1 (red) is the maximum compressive stress and σ_3 (blue) is the least compressive stress.

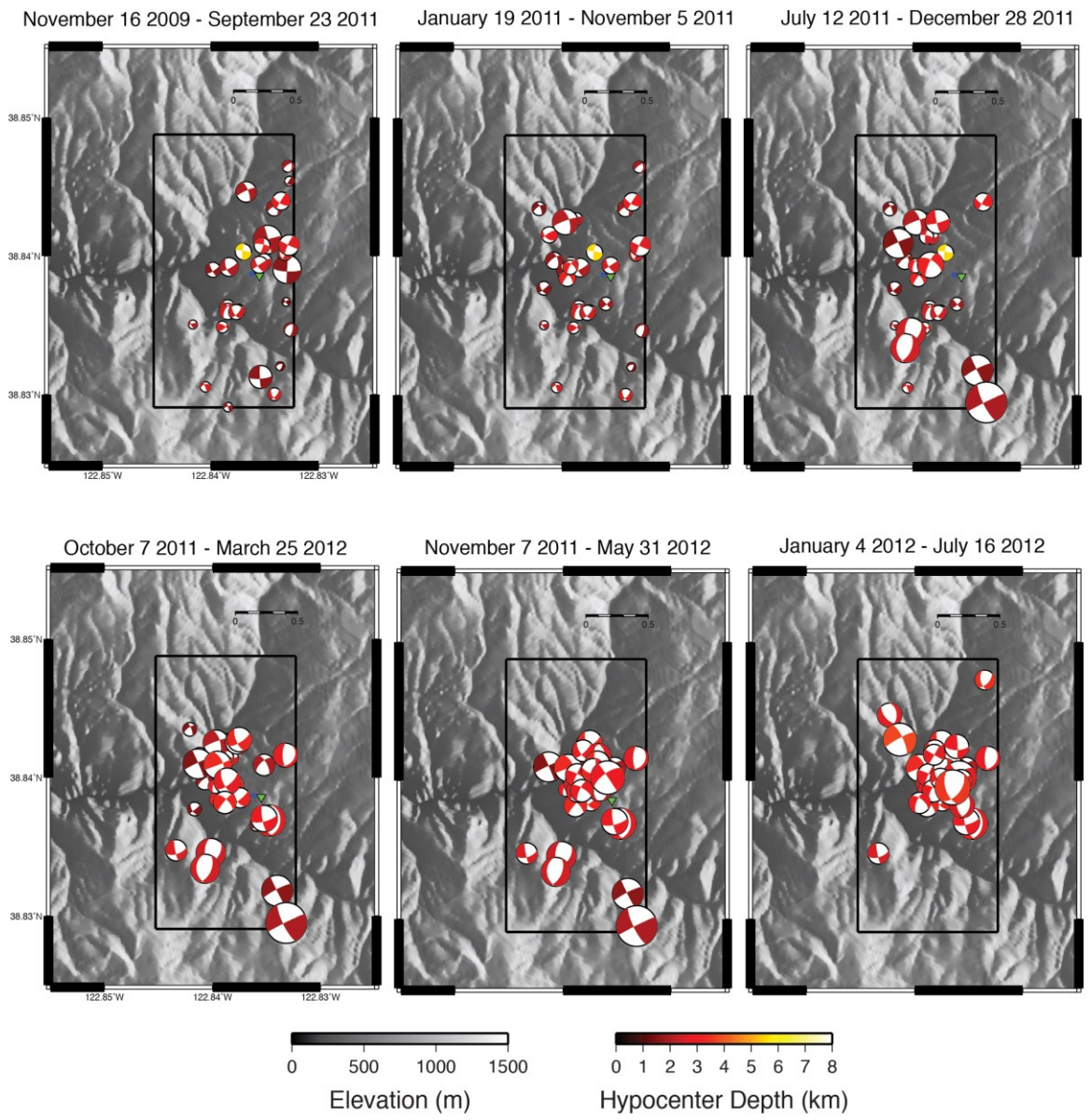

Figure 7: Moment tensor solutions for the time periods given in the respective panel titles. There are 30 moment tensors in each time window.

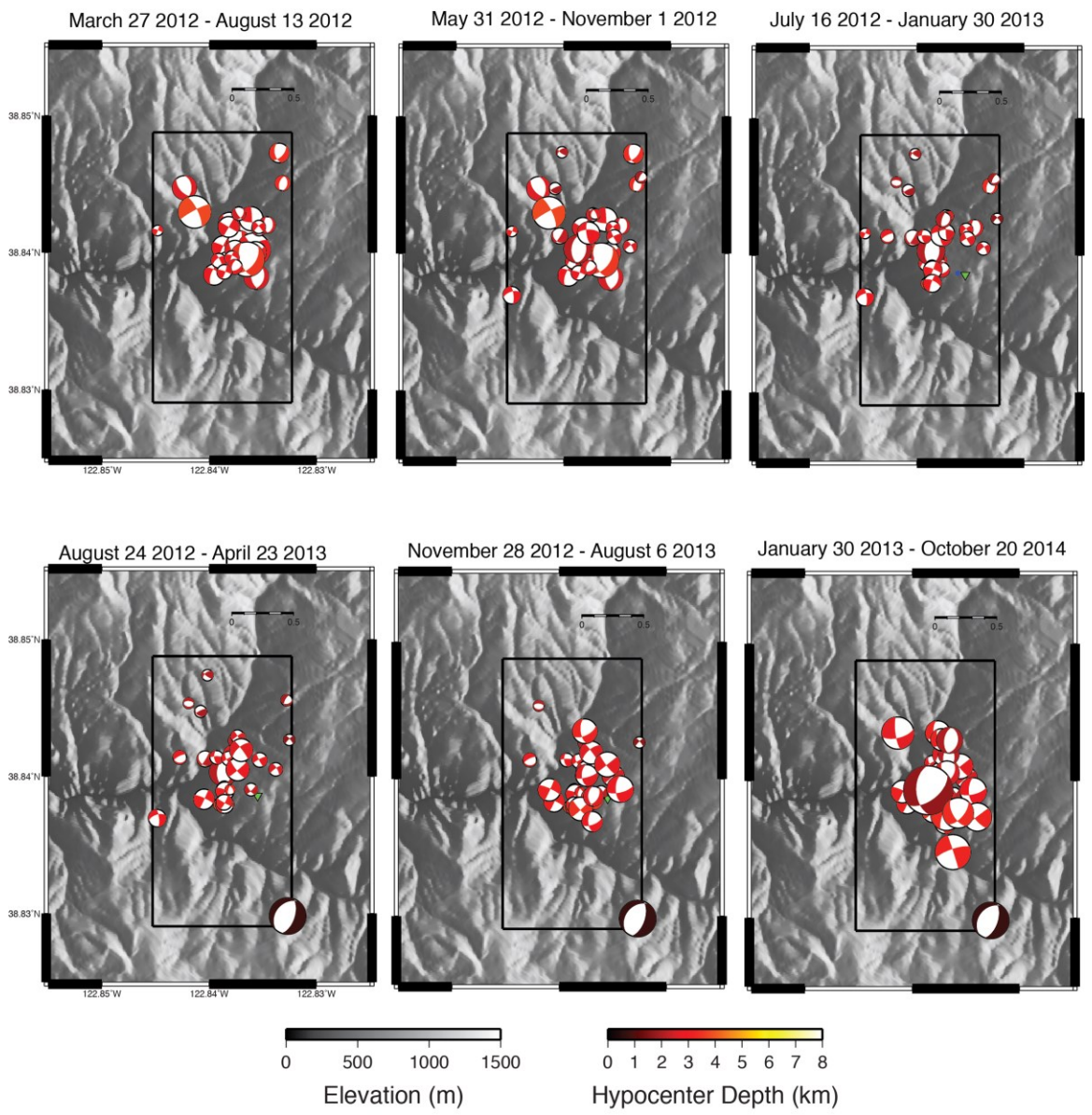

Figure 7 continued: Moment tensor solutions for the time periods given in the respective panel titles. There are 30 moment tensors in each time window.

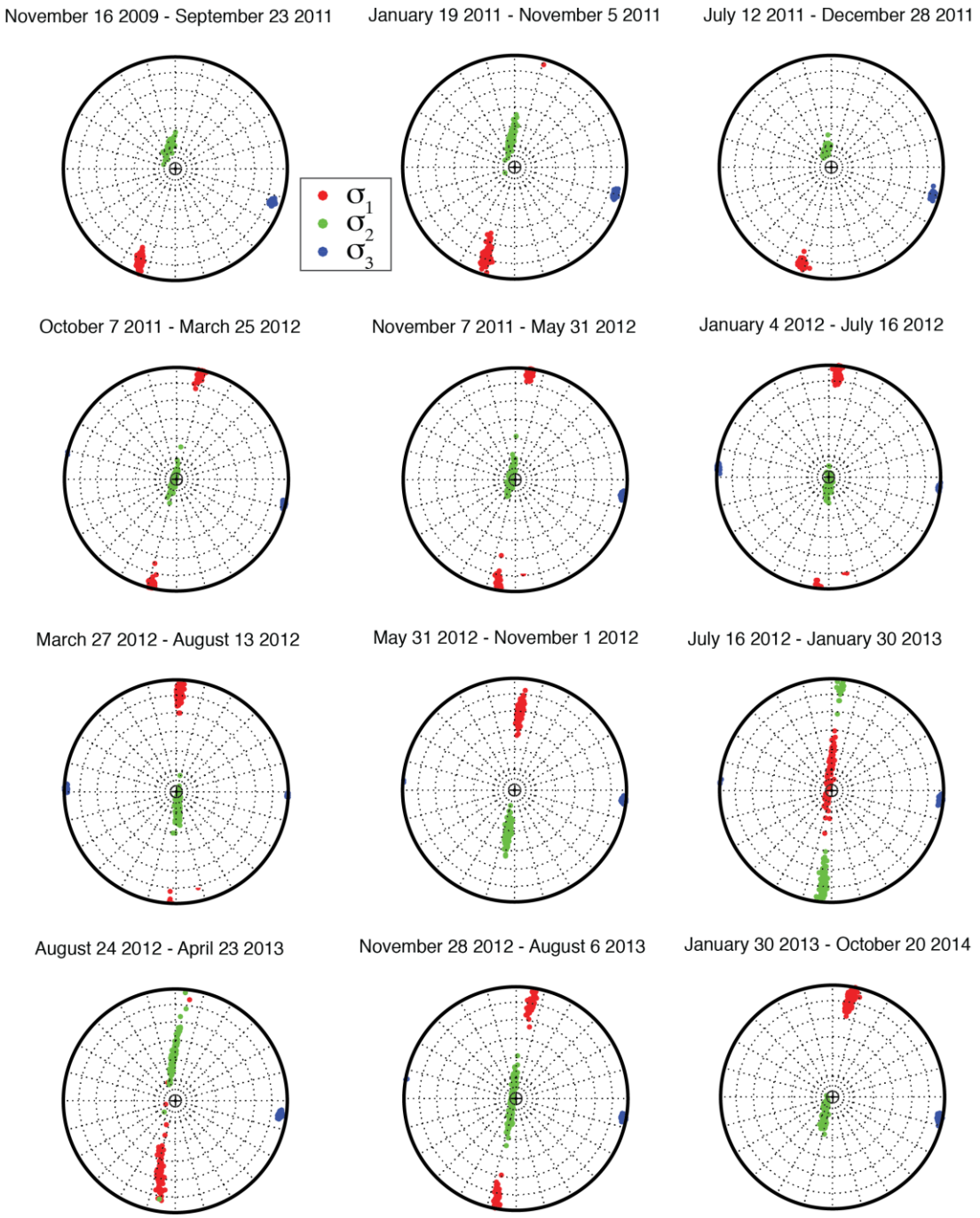

Figure 8: The orientation of in-situ stress for each of the 12 time windows. These results are from the STRESSINVERSE software (Vavrycuk, 2014).

Examining the magnitude of the stress components, it is seen that as the orientation of the stress tensor is changing so too is the shape factor, R (Gephart and Forsyth, 1984). R is defined as

$$R = \frac{\sigma_1 - \sigma_2}{\sigma_1 - \sigma_3} \tag{1}$$

where σ_1 is the maximum compressive stress and σ_3 is the least compressive stress. As can be seen in Figure 9, R decreases systematically as injection rate and total volume of injected water increases. The reduction in R is found to be due to both, a decrease in the relative magnitude of σ_3 and an increase in the relative magnitude of σ_2 indicating that the stress is evolving to a more tensile environment. The slight increase in R in time windows 6-8 (Figure 9) corresponds to the period of time when there was a hiatus in the injection of water from August 20, 2012 – January 29, 2013 and from March 12, 2013 to April 9, 2013 (Figure 2).

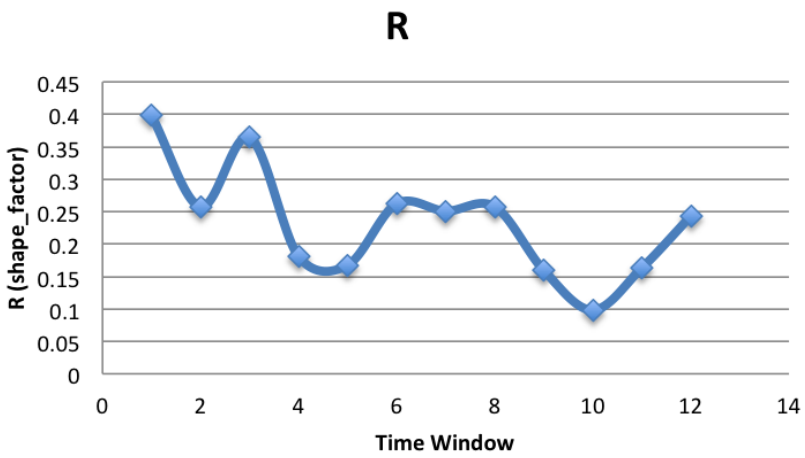

Figure 9: The stress shape factor R is plotted for the twelve time windows defined in Figure 7. R is seen to decrease systematically as water is injected.

Martinez-Garzon et al. (2013) studied the stress tensor using catalog first-motion focal mechanisms for a region just east of our study area finding a correlation between observed rotation in the stress tensor and multiple periods of high injection rate. The magnitude and direction of the rotation we observe for σ_3 is consistent with their findings. However, in their study area they found the plunge of σ_1 to decrease, whereas we observed it to increase. It is possible that there are different orientations of the initial stress tensor in localized fault bounded domains, and thus the initial stress orientation and the directions of the perturbations could differ at local scales because of the local effects of thermal cooling and increase in pore pressure. Jeanne et al. (2015) carried out numerical studies of a 9-year period spanning the Prati-9 injection and found rotations of σ_1 and σ_2 with respect to the vertical of 10-60 degrees depending on position above, below or adjacent to the well. In addition, they found rotations of SHmax of between 5 to 15 degrees clockwise. Their results are based on an assumed normal faulting initial condition with σ_1 vertically oriented. While the initial stress state in our 1x2 km area is strike-slip (σ_1 horizontal / σ_2 vertical) the amount of observed rotation of σ_1 and σ_2 with the vertical is comparable, as is the horizontal rotation of the stress tensor.

4. SUMMARY

Our results to date show that there was a marked increase in the rate of seismicity in a 1x2 km region around the Prati-32 injection well as injection commenced on October 6, 2011. We have developed a semi-automated approach to estimate seismic moment tensors of the micro-earthquakes utilizing three-component seismic waveforms in the 0.7 and 1.7 Hz frequency range for $1 \leq M < 2.8$ events and in the 0.2 and 1.0 Hz frequency range for $M \geq 2.8$ events. The approach utilizes a grid search to find the optimal alignment of the waveform data with the Green's functions for an assumed 1D seismic velocity model. It is necessary to manually check the results, and in some cases, provide additional first-motion polarity constraints to eliminate waveform cycle-shift. The result of our effort has been the compilation of a 168-event waveform-based seismic moment tensor catalog for events ranging in moment magnitude from 0.7 to 3.7. We subsequently have utilized the moment tensor catalog for the Prati-32 study area to invert for the stress tensor, and to investigate possible temporal changes resulting from the fluid injection. We have applied two approaches for inverting for the stress tensor (Martinez-Garzon et al., 2014; Vavrycuk, 2014). The results demonstrate the quality of the seismic moment tensor catalog through the relatively small uncertainties in the recovered stress tensors. We find that there is an approximate 15-degree counterclockwise rotation of σ_3, and a rotation of σ_1 toward the vertical as the injected volume of water increased. The magnitude of these rotations is consistent with other nearby empirical observations (Martinez-Garzon et al., 2013) and thermo-hydromechanical simulation results (Jeanne et al., 2015). We find that there is a systematic reduction in the stress shape factor, R, as injected volume increases, indicating an evolution toward a more tensile stress state.

REFERENCES

Boyd, O. S., D. S. Dreger, V. H. Lai, and R. Gritto (2015). A Systematic Analysis of Seismic Moment Tensor at The Geysers Geothermal Field, California, Bull. Seism. Soc. Am., 105, No. 6, doi:10.1785/0120140285.

Boyd, O. S., D. S. Dreger, and R. Gritto (2016). Analysis of In-Situ Stress During EGS Resource Development at The Geysers, CA, Annual meeting of the American Geophysical Union, S31B-2737, presented on December 14, 2016

Gephart, J.W. & Forsyth, D.W., 1984. An improved method for determining the regional stress tensor using earthquake focal mechanism data: application to the San Fernando earthquake sequence, J. Geophys. Res., 89, 9305–9320.

Gritto, R. D.S. Dreger, O.S. Boyd, and T. Taira (2016), Fluid Imaging, Moment Tensors and Finite Source Models During the EGS Demonstration Project at The Geysers, CA, 41st Workshop on Geothermal Reservoir Engineering, February 22-24, 2016, Stanford University, Stanford, CA.

Guilhem, A., L. Hutchings, D.S. Dreger and L.R. Johnson (2014), Moment tensor inversions of M~3 earthquakes in the Geysers geothermal fields, California, J. Geophys. Res., 10.1002/2013JB010271.

Gutenberg, B., Richter, C. F. (1956). Magnitude and Energy of Earthquakes. Annali di Geofisica, 9: 1–15

Hardebeck, J. L., and A. J. Michael (2004). Stress orientations at intermediate angles to the San Andreas fault, California, J. Geophys. Res. 109, no. B11303, doi: 10.1029/2004JB003239.

Hardebeck, J, A. Michael 2006, Damped regional-scale stress inversions: Methodology and examples for southern California and the Coalinga aftershock sequence, J. Geop. Res., doi:10.1029/2005JB004144.

Jeanne, P., J. Rutqvist, P. F. Dobson, J. Garcia, M. Walters, C. Hartline and A. Borgia (2015). Geomechanical simulation of the stress tensor rotation caused by injection of cold water in a deep geothermal reservoir, J. Geophys. Res. Solid Earth, 120, doi:10.1002/2015JB012414.

Martinez-Garzon, P., G. Kwiatek, M. Ickrath, and M. Bohnhoff (2014). MSATSI: A MATLAB Package for Stress Inversion Combining Solid Classic Methodology, A New Simplified User-Handling, and a Visualization Tool, Seism. Res. Lett., 85(4), 896-904, doi: 10.1785/0220130189.

Martinez-Garzon, P., M. Bohnhoff, G. Kwiatek, and G. Dresen (2013). Stress tensor changes related to fluid injection at The Geysers geothermal field, California, Geophys. Res. Lett., 40, 2596-2601, doi: 10.1002/grl.50438.

Ross, A., G. R. Foulger, and B. R. Julian (1996). Non-double-couple earthquake mechanisms at The Geysers geothermal area, California, Geophys. Res. Lett. 23, 877–880.

Vavrycuk, V. (2014). Iterative joint inversion for stress and fault orientations from focal mechanisms, Geophys. J. Int., 199, 69-77, doi: 10.1093/gji/ggu224.